Journal of Heat and Mass Transfer Research

Journal homepage: https://jhmtr.semnan.ac.ir

Semnan University

ISSN: 2383-3068

Research Article

Numerical Study of the Impact of Peritoneal Fluid and Its Convection on Magnetic Nanoparticle Hyperthermia in the Treatment of Peritoneal Metastasis

Mohadese Ranjbaran [a], Mohammad Hossein Tavakoli [a*], Zahra Keshtpour Amlashi [b], Safoora Nikzad [c*]

[a] *Department of Physics, Faculty of Science, Bu-Ali Sina University, Hamadan 65174, Iran*

[b] *Cancer Research Center, Hamadan University of Medical Sciences, Hamadan 65178, Iran*

[c] *Department of Medical Physics, Faculty of Medicine, Isfahan University of Medical Sciences, Isfahan 65178, Iran*

ARTICLE INFO

Article history:

Received: 2025-04-27

Revised: 2026-02-22

Accepted: 2026-05-09

Keywords:

Magnetic nanoparticles;

Hyperthermia;

Peritoneal metastasis;

Heat transfer;

Fluid modeling.

ABSTRACT

This study evaluates magnetic nanoparticle hyperthermia for treating peritoneal metastasis, focusing on the effect of ascitic fluid and convection on tumor heating and healthy tissue. Magnetic nanoparticles (MNPs) were applied to raise tumor temperature to 42–46°C under an alternating magnetic field. Finite element simulations were used to calculate magnetic field distribution (Maxwell's equations), heat generated by MNPs (Rosensweig model), temperature in the tumor and surrounding solid tissue (Pennes bioheat equation), and fluid temperature and convection in the peritoneal cavity (Navier–Stokes equations). Induction heating in the tumor was unaffected by ascitic fluid, though overall heat in the peritoneal cavity increased. Heat generated by MNPs was lowest at the tumor center and highest near the surface, with ascitic fluid enhancing heat production. Tumor temperature reached 45–46°C without ascitic fluid but decreased to 43–44°C when convection was present. Healthy tissue temperature remained below 44.2°C in both scenarios. Convective cooling in the fluid was the dominant factor influencing temperature distribution, causing non-uniform heating within the tumor. Conclusion: Magnetic nanoparticle hyperthermia effectively targets tumor tissue while protecting healthy tissue. The presence of ascitic fluid significantly alters temperature distribution through convection, highlighting the importance of considering fluid dynamics in treatment planning.

1. Introduction

Cancer is a leading cause of death globally, and its incidence is rising at an alarming rate. This complex disease occurs when abnormal cells multiply uncontrollably in the body [1, 2]. These cells have the ability to invade surrounding tissues and spread to other areas of the body via the bloodstream or lymphatic system, a process known as metastasis. When cancer is described as aggressive, it means that the cancer cells have infiltrated nearby tissues or other organs, resulting in the formation of metastatic tumors [3, 4]. Peritoneal metastasis usually begins with cancers of other organs, such as the gastric,

* **Corresponding author.**
E-mail address: *mht@basu.ac.ir*

Cite this article as:

Ranjbaran M, Tavakoli M. H., Keshtpour Amlashi, Z. and Nikzad, S., 2026. Numerical Study of the Impact of Peritoneal Fluid and Its Convection on Magnetic Nanoparticle Hyperthermia in the Treatment of Peritoneal Metastasis. *Journal of Heat and Mass Transfer Research*, 13(4), pp. 423-438.

https://doi.org/10.22075/JHMTR.2026.37513.1732

intestines, uterus, ovaries, or esophagus, and then spreads to the peritoneal cavity. Peritoneal cancer can occur anywhere in the abdomen and affects the outer surface of any of the abdominal organs. Metastasis is a process that propels cancer into more advanced stages, making its treatment considerably more challenging. In comparison to gastric cancer treatment, managing peritoneal metastasis is far more complex due to the widespread dispersion of cancer cells within the peritoneal cavity. As a result, the likelihood of successfully treating peritoneal metastasis is much lower than that of gastric cancer [5, 6]. Figure 1 shows peritoneal metastasis.

In most patients with peritoneal metastasis, abdominal ascites also develops. Ascites refers to the accumulation of fluid in the peritoneal cavity. It can be caused by various factors, including liver diseases, peritoneal metastasis, and gastrointestinal cancers. Furthermore, the implantation of cancer cells in the peritoneum stimulates the production and secretion of ascitic fluid [7].

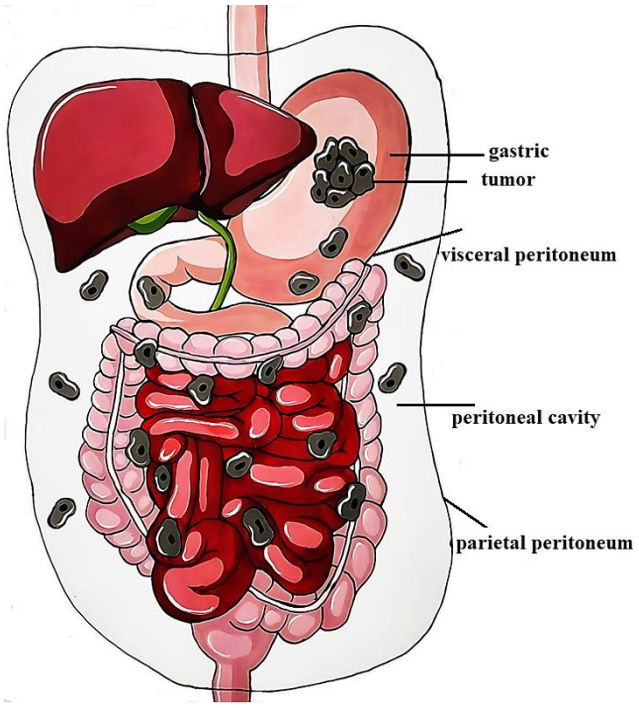

Fig. 1. Peritoneal metastasis

Common approaches to cancer treatment include chemotherapy, radiotherapy, and surgery, which are often used in combination for patients. The best cancer treatment method is one that specifically targets cancer cells (tumors) and prevents damage to healthy tissues (a non-offensive method). However, in conventional methods, this goal has not been fully achieved, and healthy tissues are also affected. One of the new and non-invasive cancer treatment methods is hyperthermia, which has recently been approved. In this method, by controlled heating of the tumor tissue to a temperature range of 42-46°C, cancer cells are destroyed. Today, hyperthermia has found extensive and diverse applications in the medical field as a complementary method alongside conventional cancer treatments [8, 9].

In hyperthermia therapy, heat can be produced through various techniques. One effective approach involves the use of magnetic nanoparticles (MNPs) in conjunction with an external alternating magnetic field (AMF) applied to the targeted region. In this method, the MNPs serve as localized heat sources, raising the temperature within the tumor tissue. Accurately analyzing the heat and temperature distribution in both the tumor and the surrounding healthy tissues is essential. Several key factors directly impact the efficiency of this process, including the frequency, intensity, and spatial distribution of the magnetic field generated by the induction coil; the physical and magnetic properties of the nanoparticles; the tumor's location; and the duration of the treatment. These elements play a critical role in achieving effective and controlled therapeutic outcomes [10, 12].

This method, by focusing heat specifically on cancerous tissues, results in fewer side effects on the surrounding healthy cells. Healthy cells typically exhibit greater resistance to elevated temperatures, whereas cancer cells are more vulnerable to heat due to their distinct metabolic and structural characteristics. As a result, magnetic hyperthermia (MHT) offers high

effectiveness in targeting and destroying cancer cells while significantly reducing harm to healthy tissues and minimizing side effects, unlike the adverse effects commonly associated with chemotherapy and radiotherapy [13].

The presence of ascites plays a key role in MHT for peritoneal metastases. Ascites, as the accumulated fluid in the peritoneal cavity, can affect the transfer and distribution of heat. Additionally, this fluid serves as an indicator for assessing disease progression and determining the suitability of the patient for treatment [14-16]. During treatment, the increase in temperature in the presence of ascites may have unforeseen effects on tissues and fluids. Therefore, a thorough examination of the characteristics of ascites and the adjustment of thermal modeling and treatment parameters are essential. Numerical analysis of the impact of ascitic fluid on the MHT process presents a new area for research. Ascitic fluid acts as a therapeutic challenge for existing treatment methods, consequently slowing down or limiting the treatment process. The presence of ascitic fluid can affect the distribution of heat and the effectiveness of the treatment.

Ultimately, analyses and modeling related to MHT are not only theoretically important but can also have a direct impact on improving treatment outcomes in patients with peritoneal metastasis. The use of numerical models in design, by optimizing the magnetic field and heat distribution, helps enhance the efficacy and safety of the treatment. These models aim to achieve deeper penetration and more uniform heating, reduce side effects through precise control of heat distribution, and protect healthy tissues, thereby paving the way for the creation of personalized treatment protocols for each patient. Since peritoneal metastases are usually located deep within the body and adjacent to vital structures, MHT can selectively heat these areas and focus the treatment effect solely on cancerous tissues without damaging the surrounding healthy tissues. MHT is a promising and novel method for treating peritoneal metastases, offering advantages over chemotherapy and radiotherapy with its high targeting, fewer side effects, and the possibility of combining with other treatments. However, further research is necessary to improve its efficacy and reduce costs for broader acceptance.

Although many studies have been conducted on the treatment of cancer tumors in different parts of the body with MNPs [17–20], unfortunately, due to many problems, difficulties, and obstacles, there has been little study done on peritoneal metastasis.

Matsumi et al. [21] experimentally and in the lab studied the treatment of peritoneal metastasis that had spread from gastric cancer (peritoneal metastasis of gastric cancer). The study used a mouse model with peritoneal metastasis cancer. For treatment, a hyperthermia method was used with superparamagnetic iron oxide (Fe_3O_4) nanoparticles (SPIONs). Finally, they found that MHT is a more effective treatment for peritoneal metastases than other treatment methods. Based on this study, MHT could be used as a new treatment option for peritoneal metastasis.

Rouni et al. [22] have investigated the safety of magnetic hyperthermia systems based on nanoparticles, which use controlled heat to destroy cancer cells in cancer treatment. This research focuses on evaluating the safety of a system that utilizes an AMF and MNPs to generate heat. Practical experiments and empirical data have been used to examine the impact of this system on body temperature.

Chia et al. [23] have investigated the effects of hyperthermia and its combination with intraperitoneal drug delivery in the treatment of peritoneal metastases. Initially, the immune status of the healthy peritoneal cavity and the immune structure of peritoneal metastases were examined. Then, the positive and negative effects of hyperthermia and its heat shock response on the tumor immune microenvironment were analyzed. Additionally, the impact of hyperthermia on the biomechanical properties of tumor tissue and its implications for immune cell infiltration were studied.

In addition to SPIONs, numerous alternative materials have been investigated for use in magnetic hyperthermia therapy. These include various MNPs such as cobalt-based, nickel-based, and core-shell structured nanoparticles. Each of these materials exhibits distinct magnetic properties that influence their ability to generate localized heating when subjected to an AMF. The selection of an appropriate nanoparticle system is critical, as it directly affects parameters such as specific absorption rate (SAR), magnetic susceptibility, biocompatibility, and stability. These factors play a pivotal role in optimizing therapeutic efficacy, ensuring controlled thermal responses, and minimizing off-target effects during hyperthermia-based cancer treatments. For this study, SPIONs were chosen due to their enhanced effectiveness in treating peritoneal metastasis. Experimental results from Matsumi et al. [21] demonstrated that SPIONs perform exceptionally well in generating localized heat under AMF exposure, making them highly suitable for targeting metastatic tumors, particularly in sensitive regions like the peritoneum. Their ability to specifically heat

tumor cells while causing minimal damage to adjacent healthy tissue significantly improves the overall therapeutic efficacy.

Recent research has shown that peristaltic blood flow and nanofluids, including hybrid and TiO_2/water-based fluids, can strongly affect the distribution of nanoparticles, heat transfer, energy storage, and overall flow characteristics. Factors such as thermal effects, squeezing and rotational motions, as well as external influences like electroosmotic or magnetic fields, allow for precise control over particle accumulation and temperature uniformity. Additionally, the shape and geometry of nanoparticles play a key role in directing energy and drug delivery to targeted regions. These analytical and numerical studies offer a solid theoretical foundation for optimizing magnetic hyperthermia treatments and improving therapeutic outcomes [24-29].

This research has focused on modeling hyperthermia using MNPs for the treatment of cancer that starts in the gastric area and metastasizes to the peritoneum. This metastasis leads to the accumulation of ascitic fluid in the peritoneal cavity, and the effect of the presence of ascitic fluid on this therapeutic process has been examined. This study was conducted to achieve the desired temperature in the target area (tumor).

This study evaluates the effect of hyperthermia with MNPs in the treatment of peritoneal metastases and examines the role of ascitic fluid in the peritoneal cavity on the distribution of the magnetic field and the heat generated during the treatment process. The aim of this study is to investigate and find the best treatment for these patients and achieve a uniform temperature distribution in the tumor so that all cancer cells are destroyed without damaging the surrounding healthy tissue.

The main innovation of this article is the numerical analysis and simulation of the impact of the presence and absence of ascites in MHT, providing new data. Additionally, this study can play a significant role in the optimal design of therapeutic protocols. These findings significantly contribute to the development of more effective methods for addressing challenges such as the presence of ascites and complex tumor conditions. Optimizing treatment parameters can help reduce damage to the healthy tissues surrounding the tumor. The results of this research are not only applicable in the treatment planning of patients with peritoneal metastasis but can also serve as a model for designing similar treatments for other cancers with deep tissue tumors or abdominal tumors in various locations. This approach, by improving treatment efficacy, reducing side effects, and providing accurate predictions of treatment outcomes, enables widespread use in scientific research and clinical applications.

Simulations and results indicate that the presence of ascites in the peritoneal cavity has a significant impact on temperature distribution, while ascitic fluid, which is usually considered an obstacle in other therapeutic methods such as radiotherapy, can be treated with this method without causing serious hindrance. Since MHT has fewer side effects and can be combined with other therapeutic methods, it is introduced as a targeted and precise treatment for deep tumors, especially in individuals with advanced peritoneal cancer accompanied by abdominal ascites.

The selection of this numerical model is particularly important due to the complex anatomical and physiological characteristics of peritoneal metastasis. Traditional hyperthermia models often assume homogeneous tissues and neglect the presence of fluid, whereas this approach simultaneously accounts for electromagnetic field distribution, heat generation by nanoparticles, bioheat transfer in solid tissues, and fluid convection. Since ascitic fluid commonly occurs in advanced stages, ignoring it can lead to unrealistic temperature estimates. By integrating Maxwell's equations, Rosensweig's model, the Pennes bioheat equation, and the Navier–Stokes equations, this model provides a more realistic depiction of treatment conditions and enhances the accuracy of temperature predictions for patients with peritoneal metastasis and ascitic fluid.

2. Mathematical Model

Figure 2 is an image of the geometry of the model. As can be seen, the model that was studied is a two-dimensional (2D) model that includes an induction coil, abdominal tissue, and a spherical tumor in the gastric tissue that eventually metastasizes into the peritoneum. Therefore, AMF is applied to the target tissue (the tumor), and the MNPs in the tumor act as a source of heat generation.

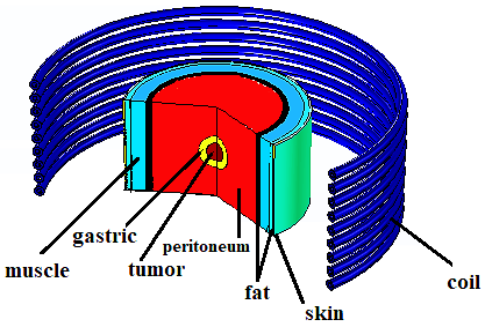

Fig. 2. View of the geometrical model used for MHT

Model assumptions used are:

1. The system is linear, isotropic, and stationary.
2. All materials are non-magnetic and have no net electric charge except MNPs inside the tumor.
3. The displacement current density is neglected, and the electric current distribution inside the coil is assumed to be uniform.
4. The system has rotational symmetry around the z-axis.
5. The distribution of MNPs in the tumor is uniform.

Although analytical solutions can be applied to simplified bioheat or electromagnetic models, such approaches are generally limited to homogeneous domains, simplified geometries, uniform heat generation, and purely conductive heat transfer conditions. In the present study, the problem involves the coupled interaction of electromagnetic field distribution, heat generation by magnetic nanoparticles based on Rosensweig's theory, bioheat transfer in heterogeneous biological tissues, and natural convection of ascitic fluid governed by the Navier–Stokes equations. Due to geometric complexity, spatial variation of material properties, and nonlinear convection effects, deriving a closed-form analytical solution would require significant simplifications that reduce physiological realism. Therefore, the finite element method was adopted to accurately solve the coupled electromagnetic–thermal–fluid problem.

2.1. Induction Heating

In the process of induction heating, the alternating current in the coil generates time-dependent electromagnetic fields in the space around the coil. When a workpiece or electrically conductive (like a human body) object is placed in these fields, eddy currents are generated, and the Joule effect (RI^2) causes heat to be generated. By solving Maxwell's equations and using the vector potential equation with the magnetic field $\left(\vec{B} = \nabla \times \vec{A}\right)$ and Joule heating, the induced heat generated in the tissue is obtained from the following equation:

$$Q = \frac{|-i\omega\sigma A_0|^2}{2\sigma} \tag{1}$$

where ω is the angular frequency. σ is the electrical conductivity of the tissue. A_0 is the complex amplitude of the vector potential [30].

2.2. Heat Generated by MNPs

Heat generation by MNPs is obtained as follows [31]:

$$P = \mu_0 \pi x_0 f H^2 \frac{2\pi f \tau_{eff}}{1 + (2\pi f \tau_{eff})^2} \tag{2}$$

where P, μ_0, x_0, f and H are the power dissipation of MNPs per unit volume, the permeability of free space, equilibrium susceptibility, the frequency of the applied magnetic field, and the magnetic field intensity, respectively. The effective relaxation time in Eq. (2), τ_{eff} can be described as follows:

$$\tau_{eff} = \frac{\tau_B \tau_N}{\tau_B + \tau_N} \tag{3}$$

where τ_B is the Brownian relaxation time, τ_N is Néel relaxation time, τ_B is defined as follows:

$$\tau_B = \frac{3\eta V_H}{K_B T} \tag{4}$$

where η, K_B and T are the viscosity of the suspension, the Boltzmann constant, and the absolute temperature of MNPs, respectively. V_M is the volume of MNPs without including their shell. Because of the MNPs' spherical volume, it is defined as $V_M = \frac{\pi \mathrm{D}^3}{6}$. V_H is the volume of the MNPs with a shell. It is defined as $V_H = \frac{\pi(D+2\delta)^3}{6}$. where D and δ are the diameter of MNPs and the thickness, respectively. The equation for the Néel relaxation time is:

$$\tau_N = \frac{\sqrt{\pi}}{2} \tau_0 \frac{e^{\Gamma}}{\sqrt{\Gamma}} \tag{5}$$

where K_{eff} is the anisotropy constant, $\tau_0 = 10^{-9} s$ is the attempt time, and $\Gamma = \frac{K_{eff} V_M}{k_B T}$. The equilibrium susceptibility X_0 in the Langevin equation expresses it as follows:

$$x_0 = x_i \frac{3}{\zeta} (\coth(\zeta) - \frac{1}{\zeta} \tag{6}$$

where $\mathrm{x_i}$ and ζ are the initial susceptibility and the Langevin parameter, respectively. x_i described as follows $x_i = \frac{\mu_0 \phi M_d^2 V_M}{3 k_B T}$ and ζ explained as follows:

$$\zeta = \frac{\mu_0 M_d H V_M}{K_B T} \tag{7}$$

where M_d and ϕ are the domain magnetization of suspended MNPs and the volume fraction of MNPs, respectively.

2.3. Heat Transfer in Solid Tissues

To get the temperature distribution during hyperthermia, using Pennes bio-heat transfer equations for healthy tissue and tumor tissue, the

following relationships are used, respectively [32]:

$$\rho_1 c_1 \frac{\partial T}{\partial t} = \nabla.(k\nabla T) + \rho_b c_b \omega_b (T_a - T) + Q_{met} \quad (8)$$

$$\rho_2 c_2 \frac{\partial T}{\partial t} = \nabla.(k\nabla T) + \rho_b c_b \omega_b (T_a - T) + Q_{met} + P \quad (9)$$

where $\rho_1, \rho_2, \rho_b, c_1, c_2, c_b, k, T_a, T, \omega_b, Q_{met}$ and P are the tissue density, the tumor density, the blood density, the specific heat of the tissue, the specific heat of the tumor, the specific heat of blood, the thermal conductivity of the tissue, the tissue temperature, and the arterial blood temperature, the blood perfusion rate, the metabolic heat source, and the power dissipation of MNPs per unit volume in the tumor, respectively.

The considered boundary conditions for Pennes bio-heat transfer equations are as follows:

1) On the upper and lower boundaries of the desired model, the heat flux is zero ($\frac{\partial T}{\partial n} = 0$).
2) The temperature on the body surface is considered to be 37 °C.

In the thermal model based on the Pennes equations, zero heat flux is applied at the upper and lower boundaries of the computational domain, while the external body surface temperature is maintained at 37 °C. Continuity of temperature and heat flux is ensured across all internal tissue interfaces. When ascitic fluid is present, a no-slip condition is applied at the tumor surface and at the inner wall of the peritoneal cavity. Blood perfusion and metabolic heat generation are neglected within the fluid region.

2.4. Fluid Modeling

The fluid flow in the peritoneal cavity has been modeled using the Navier-Stokes equations with the Boussinesq approximation, which in the steady state is as follows:

$$\rho\nabla.(vv) = \mu\nabla^2 v + \nabla p + \rho g\beta(T - T_0)e_z \quad (10)$$

The left-hand side of this equation represents the change in momentum of a fluid element with v velocity and ρ constant mass density. The right-hand side of the equation represents the forces acting on the fluid element. The first term on the right side is the friction between adjacent fluid elements, which is determined by the fluid's viscosity μ. In the calculations, the viscosity of the ascites $\mu = 0.001 Pa.s$ has been taken into account.

The second term p is the pressure difference. The third term is the volumetric force acting on the fluid element, which is derived from convection and includes g gravitational acceleration, ρ constant mass density, and β the thermal expansion coefficient. It has been taken $\beta = 3.42 \times 10^{-4} k^{-1}$ and $T_0 = 37°C$ into account in the calculations [33, 34].

In the stationary state, the heat equation for the fluid is as follows:

$$-k\nabla^2 T + \rho c(v.\nabla T) = 0 \quad (11)$$

where k, ρ, and c are the thermal conductivity, density, and heat capacity of the ascites, respectively. Similar to eqs. (8) to (10), the T temperature and v fluid element velocity are considered. To solve the equations, boundary conditions were defined such that the fluid velocity on the boundaries (the inner wall of the peritoneal cavity and the tumor surface) is considered to be zero ($v = 0$)

2.5. Solving the Equations

The finite element method has been used to solve the equations. Figure 3 shows a view of the mesh used for the calculations. The type of meshing used in the calculations is free triangular.

Due to the greater importance and intensity of temperature and heat changes in the wall and peritoneal cavity and tumor, finer meshing has been considered in these areas. Additionally, in the case where convection has been examined, a mesh of boundary layers in the tumor wall and the inner wall of the peritoneal cavity in contact with ascitic fluid has been utilized.

In the studied model, after injecting iron oxide nanoparticles Fe_3O_4 into the tumor and achieving a uniform distribution, the target tissue is placed in an AMF by coil. This coil consists of 9 rings with a circular surface and a thickness of 0.5 cm made of copper.

In order to investigate the effect of ascitic fluid on the results of nanoparticle hyperthermia simulation in peritoneal metastatic cancer, calculations have been performed for the following conditions:

Condition 1. The peritoneal cavity is assumed to be devoid of ascitic fluid.

Condition 2. Since ascitic fluid has accumulated in the peritoneal cavity during treatment in some patients, ascitic fluid is considered within the peritoneal and abdominal cavity. In this case, blood perfusion and metabolic heat in the peritoneal cavity are zero.

Figure 4 shows peritoneal metastasis with and without the presence of ascitic fluid.

For peritoneal metastasis and stomach cancer, MHT sessions usually last between 30 to

60 minutes; however, in this article, the treatment time is a fixed constant. This duration is based on the thermal dose required to destroy cancer cells (usually in the temperature range of 41-46°C) and the tolerance of healthy tissues. However, the exact treatment duration may vary depending on the specific protocols of treatment centers and the equipment used [35, 36].

In this study, to ensure the accuracy and robustness of the numerical simulations, a well-defined convergence criterion was applied. In each simulation, the solvers were iterated multiple times until the results became stable. The simulation was considered converged and reliable when the changes in the magnetic field, tissue temperature, and peritoneal fluid velocity between successive iterations became negligible. This approach ensures that the simultaneous simulations of the magnetic field, nanoparticle heating, tissue heat transfer, and peritoneal fluid convection are accurate and trustworthy.

All simulations were performed using COMSOL Multiphysics. The coupled equations for the magnetic field, nanoparticle-induced heating, and convective flow of ascitic fluid were solved simultaneously. The numerical solution employed the finite element method, with a finely discretized simulation domain. A direct solver was used, and the convergence criterion was set to ensure that residual changes became negligible, guaranteeing numerical accuracy and stability

A mesh independence study was conducted to ensure that the numerical results were not dependent on the grid size. In this study, an unstructured triangular mesh was generated over the entire computational domain, and finer elements were applied in critical regions such as the tumor and surrounding tissues, including the stomach, to improve accuracy. The results showed that further mesh refinement led to negligible changes in the computed variables. Therefore, full mesh independence was achieved, and the selected mesh configuration was considered appropriate in terms of both accuracy and computational cost.

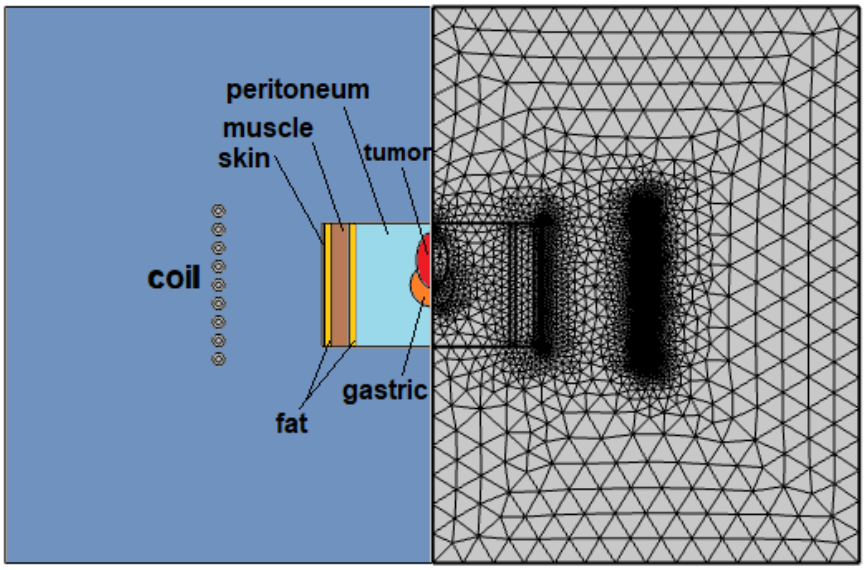

Fig. 3. Computational space (left-hand side) and its mesh for the computation (right-hand side)

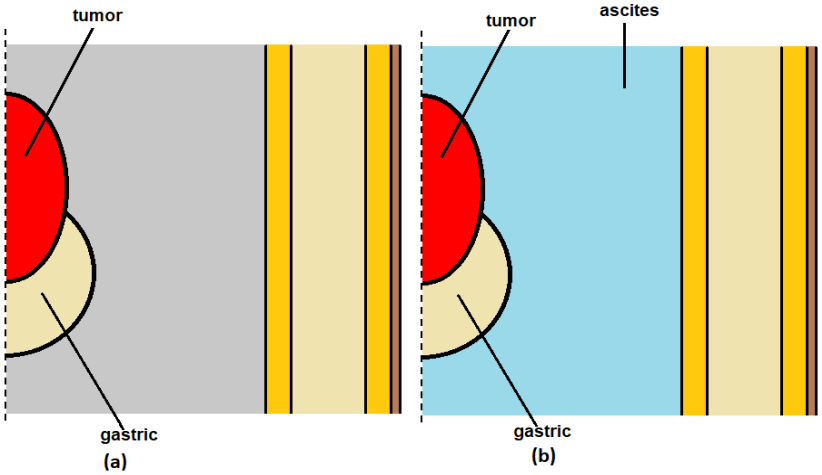

Fig. 4. Peritoneal metastatic cancer (a) without ascites and (b) with ascites examined in this study

In this study, the geometry dimensions of the model, the thermal characteristics of healthy and tumor tissue used to solve the bio-heat transfer equation, and magnetic and MNPs characteristics are presented in Table 1, Table 2, and Table 3, respectively.

Table 1. Geometry dimensions of the model

Properties (characteristic)	Value (cm)
Gastric radius	3.5
Peritoneal cavity radius	13
Muscles	3
Extraperitoneal fat and subcutaneous fat	1
Skin	0.4
The outside radius of the coil	1
inside radius of the coil The	0.5

Table 2. The thermal characteristics of healthy and tumor tissue used to solve the bio-heat transfer equation [17-21]

Parameters	Blood	Skin	Fat	Muscle	Peritoneum	Gastric	Tumor
Specific heat (J/kgK)	3770	3391	2348	3421	3600	3690	3690
Density (kg/m^3)	1060	1109	911	1090	1055	1088	1088
Thermal Conductivity (W/mK)	0.52	0.37	0.21	0.49	0.51	0.53	0.53
Blood perfusion rate (1/s)	-	0.05	0	0.00187	0.018	0.00187	0.002
Metabolic heat (W/m^3)	-	368.1	368.3	1190	5000	1190	31872

Table 3. Magnetic and MNP (Fe_3O_4) properties used in the simulation [17-20]

Parameters	Values	Unit
M_d	446	*kA/m*
K_{eff}	9	*kJ/m^3*
τ_0	10-9	S
δ	1	*nm*
k_B	1.38×10-23	*J/K*
D	19	*nm*
f	100	*kHz*
φ	0/071	-
I	100	*A*

3. Results and Discussion

In this part, the results of induction heating, heat generated by MNPs, and temperature distribution for the treatment of a human model of peritoneal metastasis cancer are presented for two cases: a) the peritoneal cavity without the presence of ascites, b) considering the ascitic fluid in the peritoneal cavity.

3.1. Induction Heating in Healthy and Tumor Tissue

In this part, the heat generated by the eddy currents (induction heating) in the tumor and healthy tissue has been calculated by the considered coil. In Fig. 5, the distribution of induced heat in healthy tissue and tumor is shown, and in Fig. 6, the distribution of induced heat in the tumor is shown.

As seen in Fig. 5, in both cases of peritoneal metastatic cancer, the highest induced heat is in the muscle. This is due to the high electrical conductivity in the muscle (0.362 S/m) compared to the skin, fat, and peritoneum. We observe that due to the skin effect, the heat decreases from the surface of the tissue towards the center of the body [37].

In Fig. 6, it is observed that the induction heating in the tumor in both cases of peritoneal metastatic cancer is similar, and the amount of induced heat generated in the tumor is very negligible. It is also observed that the amount of induction heating due to the skin effect is greater at the surface of the tumor and decreases towards the center of the tumor. It should be noted that the gradient of induced heat in the tumor is independent of the shape of the tumor and its location, and it decreases linearly towards the center of the tumor.

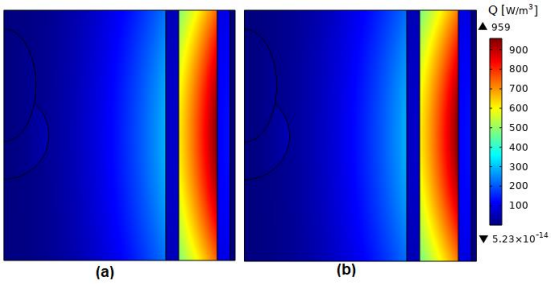

Fig. 5. The distribution of inductive heating in healthy tissue and tumor tissue: (a) in the absence of ascitic fluid and (b) in the presence of ascitic fluid

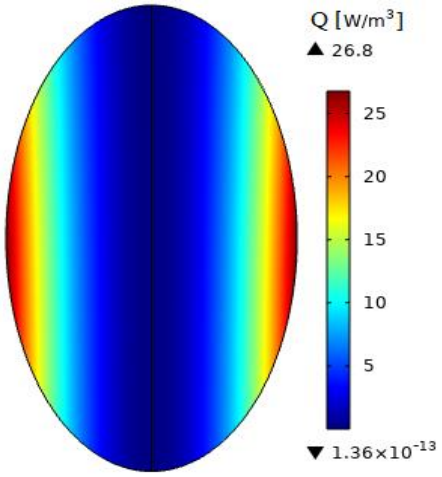

Fig. 6. The distribution of inductive heating in tumors in both ascites and non-ascites

3.2. Distribution of Heat Generated by MNPs in Tumors

In this part, we assume that MNPs are distributed only in the tumor, so the heat generated by MNPs is only inside the tumor, and this makes the tissue around the tumor remain healthy.

In Fig. 7, the heat distribution of the nanoparticle in the tumor, in two cases of peritoneal metastatic cancer with and without ascitic fluid, has been studied and presented.

Since one of the important factors in heat generation by MNPs is the intensity of the magnetic field, due to the non-uniformity of the magnetic field intensity in different parts of the tumor, the heat distribution is also different. Figure 8 shows that in both cases of peritoneal metastasis tumor, with or without ascites, the distribution of magnetic field intensity within the cancerous tissue decreases from bottom to top. The highest magnetic field intensity is located at the bottom of the tumor, near the center of the coil, because the center of the coil generates the maximum value of magnetic field intensity. Considering that the intensity of the magnetic field is one of the main factors in heat generation by MNPs (according to equation 2), the non-uniformity of the magnetic field intensity at different points in the tumor causes the distribution of the heat generation to also vary. Consequently, the intensity of the magnetic field is greater in the lower part of the tumor, and the highest amount of heat generation by MNPs is always located in this section of the tumor. (In this section, we have assumed a constant temperature to observe and analyze only the effect of the magnetic field on the generated heat).

In this part, we have considered temperature as a variable. As observed, the heat distribution of MNPs is lowest at the center of the tumor and decreases as one moves away from it, reaching its maximum value at the tumor surface. In Fig. (8b), it is observed that by considering the ascitic fluid and convection in the peritoneal cavity (case 2), the intensity of the heat generated has increased compared to case 1. This increase in the intensity of heat generation in state 2 is particularly observed in the tumor's border areas that are in contact with ascitic fluid. Therefore, it can be seen that the presence of ascites and convection within it leads to an increase in the intensity of heat in the tumor. In this part, we have considered temperature as a variable. As observed, the heat distribution of MNPs is lowest at the center of the tumor and decreases as one moves away from it, reaching its maximum value at the tumor surface. In Fig. (8b), it is observed that by considering the ascitic fluid and convection in the peritoneal cavity (case 2), the intensity of the heat generated has increased compared to case 1. This increase in the intensity of heat generation in state 2 is particularly observed in the tumor's border areas that are in contact with ascitic fluid. Therefore, it can be observed that the presence of ascites and convection within it increases the intensity of heat in the tumor. The intensity of heat generated by MNPs in the tumor of the peritoneal cavity in Fig. (8a), assumed to be devoid of ascitic fluid (case 1), has decreased compared to case 2.

The difference in the distribution of the heat generated by MNPs in the tumor in two cases is due to the dependence of the heat generated by MNPs on temperature changes and the magnetic field (Section 2-2). Since the magnetic field for a type of tumor is the same in both cases, the results indicate that the temperature distribution in the tumor will differ in the two cases examined (discussed in the next section).

By comparing Figs. 6-8, it is observed that the amount of induced heat in the tumor is much less than the amount of heat generated by the MNPs. According to calculations, since the induced heat is negligible compared to the heat generated by the MNPs, the heat of the MNPs can be considered as the total heat generated (Table 4).

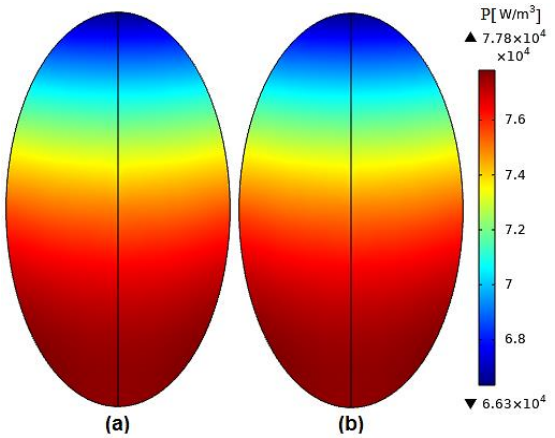

Fig. 7. Heat distribution in peritoneal metastasis for the state (a) absence of ascitic fluid; (b) presence of ascitic fluid. (Approximate constant temperature)

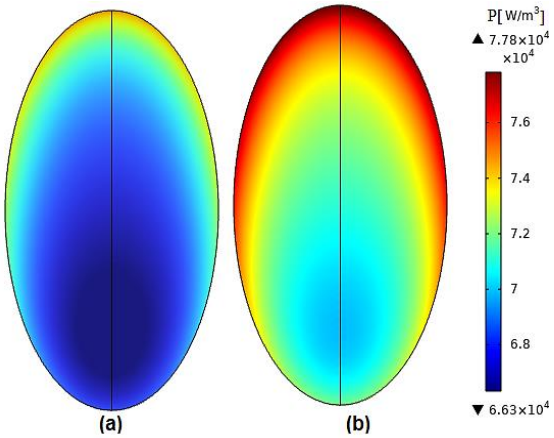

Fig. 8. Heat distribution in peritoneal metastasis for the state (a) absence of ascitic fluid; (b) presence of ascitic fluid. (Temperature variable)

Table 4. Total heat in peritoneal metastasis

The heat of MNPs with ascites (W)	The heat of MNPs without ascites (W)	Induction heating (W)
52.5	31.8	2.3×10^{-6}

3.3. Temperature Distribution in Healthy and Tumor Tissue

As mentioned, in order to examine heat transfer and obtain the temperature distribution, the Pennes equations (Equations 8 and 9) are used for healthy tissue and tumors, and the Navier-Stokes and heat equations in fluid (Equations 10 and 11) are used for ascitic fluid. The temperature distribution in the tumor is shown in Fig. 9, and the temperature distribution in healthy tissue and tumor is shown in Fig. 10.

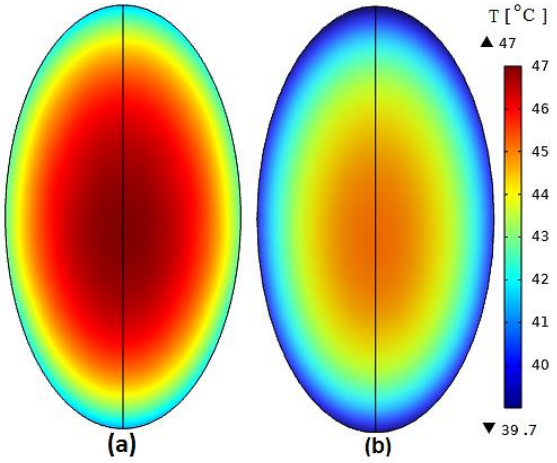

Fig. 9. Temperature distribution in peritoneal metastasis tumor for the state (a) absence of ascitic fluid; (b) presence of ascitic fluid

To more accurately evaluate the temperature distribution and better compare the models, the tumor temperature distribution curves along the symmetry axis for the two cases examined in this study are presented in Fig. 11. The results show that in the case where ascitic fluid is present in peritoneal metastatic cancer, the temperature field has decreased due to the consideration of convection in the ascitic fluid and its cooling effect, compared to the first case (without ascitic fluid).

As observed, the temperature at the center of the tumor is the highest and decreases as one moves away from the center (due to heat transfer from the surrounding area). The temperature in areas far from the tumor is 37°C. Around the tumor, in the peritoneum, the temperature rises slightly, but this increase is not enough to damage healthy tissue (less than 45°C) [38, 39]. This desirable feature of MHT localizes the heat and prevents damage to the surrounding tissue.

Cancer cells have less resistance and tolerance to sudden temperature changes compared to healthy tissue; therefore, cancerous tumors can be destroyed [11].

As shown in Figs 9 and 10, the temperature of the cancerous tissue is within the treatment temperature range. Now, the possibility of damage to the healthy tissues adjacent to the tumor must be examined.

Studies show that when the temperature exceeds 45°C, tissue damage occurs and cell death happens [40]. The computational results obtained indicate that the temperature of the healthy tissue surrounding the tumor reaches a maximum of 44.2°C, which suggests that no damage is inflicted on the healthy tissue surrounding the tumor during the hyperthermia process (Fig. 12).

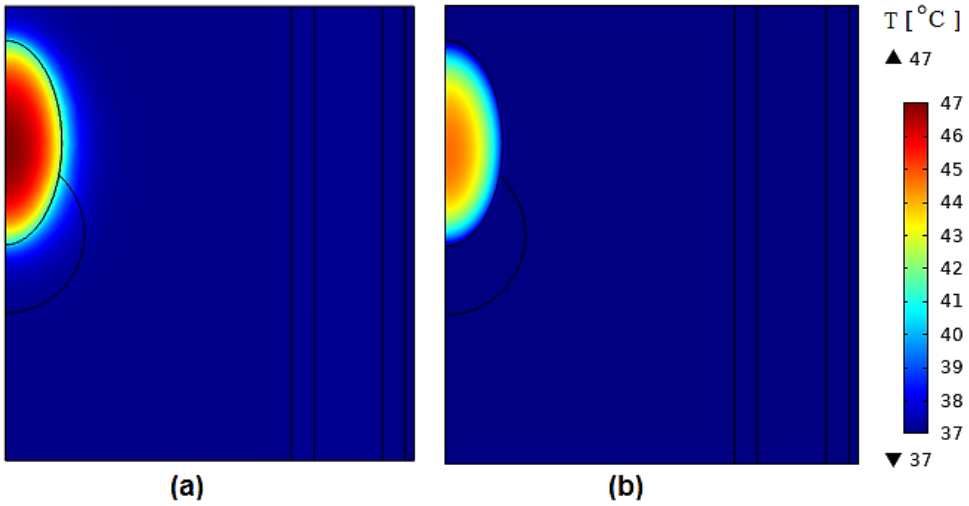

Fig. 10. Temperature distribution in peritoneal metastasis tumor and healthy tissue for the state (a) absence of ascitic fluid; (b) presence of ascitic fluid

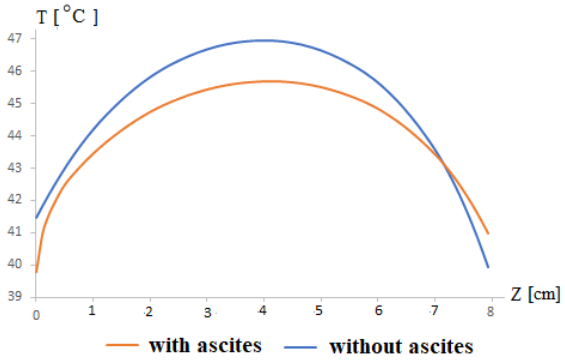

Fig. 11. Temperature distribution curves along the tumor's symmetry axis of peritoneal metastasis, along the tumor's vertical diameter

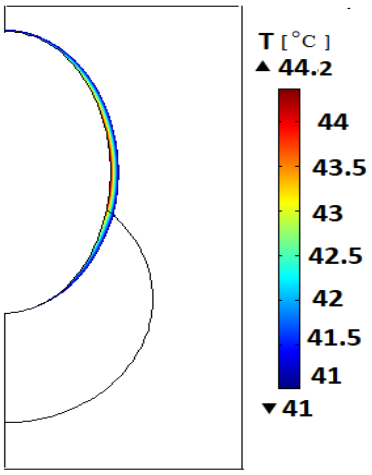

Fig. 12. Distribution of temperature in healthy tissue surrounding the tumor in the metastatic state

Figure 13 shows the flow lines of ascitic fluid. As observed, the density of the flow lines is greater in the areas adjacent to the tumor (the heat source) and decreases as one moves away from these areas. The direction of the flow, which is part of the ascitic fluid adjacent to the tumor, moves towards the upper part of the peritoneal cavity due to the increase in temperature and the resulting decrease in density.

Then, the ascitic fluid with a lower temperature and higher density moves downward. This displacement creates a large rotational cell above the peritoneal cavity and adjacent to the tumor. Additionally, a smaller counter-rotational cell forms at the lower part of the peritoneal cavity. The convective flow in ascites continues during treatment as long as the tumor temperature is higher than the surrounding tissue temperature. As we have seen, the presence of convection in the ascitic fluid causes the temperature of the tumor and its surrounding tissue to decrease.

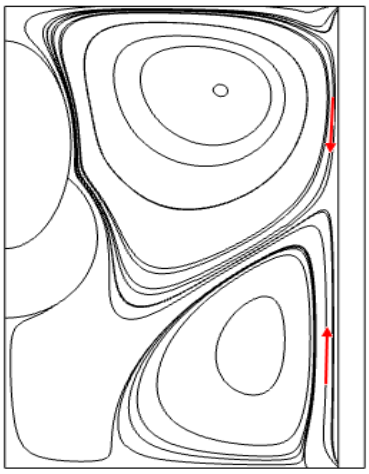

Fig. 13. Flow lines of ascitic fluid (velocity field)

4. Discussion and Validation with Experimental Studies

Previous studies have limitedly demonstrated the effectiveness of MHT in treating peritoneal metastasis. Matsumi et al. reported that SPIONs are more effective than conventional therapies in

managing peritoneal metastases originating from gastric cancer. Rouni et al. [22] evaluated the safety and thermal impact of MHT systems, showing strong alignment between experimental data and numerical simulations. Chia et al. [23] highlighted how elevated temperatures enhance immune cell infiltration into tumors, improving therapeutic outcomes.

Building upon these findings, the present study goes a step further by incorporating environmental factors, particularly the presence of ascitic fluid, into the MHT treatment model. While ascites is often a challenge in traditional therapies, our simulations indicate that MHT remains effective in such conditions. The comparison of our numerical results with the experimental and clinical data from previous studies confirms the reliability and accuracy of our model.

In contrast, the present study focuses on the influence of environmental factors, such as the presence of ascitic fluid in the peritoneal cavity, on the performance of MHT. In this study, we successfully achieved the therapeutic temperature range of 41 to 45°C, which is sufficient for cancer cell destruction. Through numerical simulation, our findings indicate that factors like fluid accumulation significantly impact heat distribution and treatment efficiency. The comparison of our results with previous studies, including those by Matsumi et al. [21], Rouni et al. [22], and Chia et al. [23], suggests that while MHT is an effective treatment approach, considering environmental factors is crucial for optimizing its therapeutic potential. The integration of these findings can contribute to the development of more effective treatment strategies for peritoneal metastasis.

These studies confirm that magnetic hyperthermia is a promising and safe cancer treatment approach. However, further research is required to refine treatment protocols, optimize parameters for different cancer types, and explore its potential in combination with therapies such as chemotherapy and immunotherapy. Future studies should focus on advanced modeling, extensive clinical validation, and in-depth investigations into the biological mechanisms of MHT to maximize its therapeutic efficacy.

The results were critically analyzed in relation to the main objective of this study, which was to investigate the effect of ascitic fluid and its convection on temperature distribution during magnetic nanoparticle hyperthermia. The simulations indicate that the presence of ascitic fluid significantly affects the thermal response of the tumor and surrounding tissues due to convective heat transfer. While the proposed model accounts for coupled electromagnetic fields, heat generation by nanoparticles, bioheat transfer, and fluid flow, it is limited to a two-dimensional framework and assumes a uniform distribution of nanoparticles within the tumor. Notably, despite the increased heat generation in the presence of ascitic fluid, the tumor temperature decreases due to enhanced convective cooling, reflecting the interaction between heat production and heat removal. These findings provide a detailed numerical assessment under ascitic conditions, while further developments, such as extending the analysis to three dimensions and considering non-uniform nanoparticle distributions, would enhance the clinical relevance of the model.

The findings of this study highlight the role of magnetic nanoparticles in enhancing heat transfer during hyperthermia treatments. Beyond numerical simulations, these nanoparticles have practical applications in clinical hyperthermia for precise tumor heating, targeted drug delivery, improved medical imaging, and other biomedical procedures requiring controlled thermal management. Including these real-world applications strengthens the study's relevance and potential impact.

5. Conclusions

In this paper, the effect of ascitic fluid and the convection caused by it on the MHT in peritoneal metastatic cancer was examined. For this purpose, a numerical study of the magnetic hyperthermia process with Fe_3O_4 nanoparticles was conducted in two states: with and without the ascites. The equations were calculated using the finite element method in a two-dimensional (2D) model. The results showed that:

1. The presence of ascitic fluid does not affect the induction heating in the tumor, but it increases the amount of induced heat in the peritoneal cavity.
2. The heat generated by MNPs (which are localized in the tumor in this hyperthermia method) is lowest at the center of the tumor and increases as one moves away from the center, reaching its maximum at the surface of the tumor. The presence of ascitic fluid in the peritoneal cavity increases the intensity of the heat generated by the MNPs in the tumor.
3. The temperature is highest at the center of the tumor and decreases as one moves away from the center.
4. The presence of convection in the ascitic fluid causes a decrease in temperature in the tumor and surrounding healthy tissue.

5. The effect of temperature reduction due to convection in ascitic fluid predominates over other effects in the peritoneal cavity.
6. Simulations indicated that the tumor temperature reached 45–46 °C when ascitic fluid was absent, while the presence of ascites reduced it to 43–44 °C due to convective cooling. Temperatures in the surrounding healthy tissue remained below 44.2°C, staying under the threshold for thermal damage. These findings support both the effectiveness of magnetic nanoparticle hyperthermia and the safety of the proposed treatment, while also emphasizing the notable impact of ascitic fluid on temperature distribution.

As a result, it can be said that in MNH in peritoneal metastatic cancer, the presence of ascitic fluid (lack of blood perfusion and convection) leads to an increase in heat intensity, a decrease in temperature, and an uneven distribution of heat in the tumor, as well as a decrease in temperature in the surrounding tissue. This decrease in temperature keeps the surrounding tissue healthy, but it can reduce the treatment effect by lowering the tumor temperature. By increasing the amount of input electrical current to the coil, the tumor can be placed in a destructive temperature range without damaging the surrounding healthy tissue.

Therefore, considering the significant effect of ascitic fluid on temperature distribution, in order to more accurately predict experimental results, it is necessary to take into account the presence of ascitic fluid in the peritoneal cavity in simulations related to nanoparticle hyperthermia in peritoneal metastatic cancer.

Nomenclature

c_1	Specific heat of the tissue
c_2	Specific heat of the tumor
c_b	Specific heat of blood
D	Diameter of MNPs
f	Frequency of the applied magnetic field
H	Magnetic field intensity
k	Thermal conductivity of the tissue
K_B	Boltzmann constant
K_{eff}	Anisotropy constant
M_d	Domain magnetization of suspended MNPs
P	Power dissipation of MNPs per unit volume
T	Absolute temperature of MNPs
T	Tissue temperature
T_a	Arterial blood temperature
V_H	Volume of the MNPs with a shell
V_M	Volume of MNPs without including their shell
x_i	Initial susceptibility
x_0	Equilibrium susceptibility

Greek symboles

μ_0	Permeability of free space
τ_{eff}	Effective relaxation time
τ_B	Brownian relaxation time
ζ	Langevin parameter
ϕ	Volume fraction of MNPs
ρ_1	Tissue density
ρ_2	Tumor density
ρ_b	Blood density
ω_b	Blood perfusion rate
Q_{met}	Metabolic heat source
μ	Fluid's viscosity
v	Velocity
ρ	Constant mass density
τ_N	Néel relaxation time
η	Viscosity of the suspension
δ	Thickness of MNPs

Funding Statement

The authors appreciate the Bu-Ali Sina University for financial support through the Grant number 1002763.

Conflicts of Interest

The author declares that there is no conflict of interest regarding the publication of this article.

Authors Contribution Statement

Mohadese Ranjbaran: Formal Analysis, Visualization, Roles/Writing – Original Draft.

Mohammad Hossein Tavakoli: Conceptualization, Methodology, Project administration, Writing – Review & Editing.

Zahra Keshtpour Amlashi: Data Curation, Supervision, Writing – Review & Editing.

Safoora Nikzad: Data Curation, Supervision, Writing – Review & Editing.

References

[1] Siegel, R. L., Miller, K.D., Wagle, N.S., Jemal, A., 2023. Cancer statistics. *CA: A Cancer Journal for Clinicians*, 73(1), pp. 17–48. https://doi.org/10.3322/caac.21763

[2] Sudhakar, A., 2009. History of cancer: ancient and modern treatment methods. *Journal of Cancer Science and Therapy*, 1, p. 1. doi:10.4172/1948-5956.100000e2

[3] Valastyan, S., Weinberg, R.A., 2011. Tumor metastasis: molecular insights and evolving paradigms. *Cell*, 147, pp. 275-292. DOI: 10.1016/j.cell.2011.09.024

[4] Noori Daloii, M.R., Fazilati, H., Tabrizi, M., 2013. Cancer metastasis: genetic and microenvironmental factors of distant tissue: a review article. *Tehran University Medical Journal*, 70, pp.671-683.

[5] Cortés-Guirial, D., Hübner, M., Alyami, M., Bhatt, A., Ceelen, W., Glehen, O., Lordick, F., Ramsay, R., Sgarbura, O., Speeten, K.V., Turaga, K.K., Chand, M., 2021. Primary and metastatic peritoneal surface malignancies. *Nature Reviews Disease Primers*, 7, p. 91. DOI: 10.1038/s41572-021-00326-6

[6] Coccolini, F., Gheza, F., Lotti, M., Virzi, S., Iusco, D., Ghermandi, C., Melotti, R., Baiocchi, G., Giulini, S.M., Ansaloni, L., Catena, F., 2013. Peritoneal carcinomatosis. *World Journal of Gastroenterology*, 19(41), pp. 6979-6994. https://doi.org/10.3748/wjg.v19.i41.6979.

[7] Rahman, G.A., Johnson, A.-W.B.R., 2001. Giant omental cyst simulating ascites in a Nigerian child: case report and critique of clinical parameters and investigative modalities. *Annals of Tropical Paediatrics*, 21, pp. 81-85.

[8] Rao, W., Deng, Z.S., 2010. A review of hyperthermia combined with radiotherapy/chemotherapy on malignant tumors. *Critical Reviews in Biomedical Engineering*, 38(1), pp. 1-22. doi:10.1615/CritRevBiomedEng.v38. i1.80

[9] Hedayatnasab, Z., Abnisa, F., Wan Daud, W., 2017. Review on magnetic nanoparticles for magnetic nanofluid hyperthermia application. *Materials and Design*, 123, pp. 174-196. doi: 10.1016/j.matdes.2017.03.036

[10] Darvishi, V., Navidbakhsh, M., Amanpour, S., 2022. Heat and mass transfer in the hyperthermia cancer treatment by magnetic nanoparticles. *Heat and Mass Transfer*, 58, pp. 1029–1039. doi: 10.1007/s00231-021-03161-3

[11] Peiravi, M., Eslami, H., Ansari, M., Zare-Zardini, H., 2022. Magnetic hyperthermia: Potentials and limitations. *Journal of the Indian Chemical Society*, 99, pp. 100269. doi: 10.1016/j.jics.2021.100269

[12] Rajan, A., Sahu, N. K., 2020. Review on magnetic nanoparticle-mediated hyperthermia for cancer therapy. *Journal of Nanoparticle Research*, 22, pp. 319. doi:10.1007/s11051-020-05045-9

[13] Gavilan, H., Avugadda, S. K., Fernandez-Cabada, T., Soni, N., Cassani, M., Mai, B. T., Chantrell, R., Pellegrino, T., 2021. Magnetic nanoparticles and clusters for magnetic hyperthermia: optimizing their heat performance and developing combinatorial therapies to tackle cancer. *Chemical Society Reviews*, 50, pp.11614–11667. https://doi.org/10.1039/D1CS00427A

[14] Berger, J.M., Preusser, M., Berghoff, A.S., Bergen, E.S., 2023. Malignant ascites: Current therapy options and treatment prospects. *Cancer Treatment Reviews*, 121, p. 102646. https://doi.org/10.1016/j.ctrv.2023.102646

[15] Sangisetty, S. L., Miner, T. J., 2012. Malignant ascites: A review of prognostic factors, pathophysiology and therapeutic measures. *World Journal of Gastrointestinal Surgery*, 4, pp. 87-95. doi: 10.4240/wjgs.v4.i4.87

[16] Ikegami, T., Ishiki, H., Kadono, T., Ito, T., Yokomichi, N., 2024. Narrative review of malignant ascites: epidemiology, pathophysiology, assessment, and treatment. *Annals of Palliative Medicine*, 13. doi: 10.21037/apm-23-554

[17] Bobade, R. S., Yadav, Sh. K., 2017. Lateral forces in the helical compression spring. *International Journal for Research in Applied Science & Engineering Technology*, 98.

[18] Misron, N., Ying, L. Q., Firdaus, R. N, Abdullah, N., Mailah, N. F, Wakiwaka, H., 2011. Effect of Inductive Coil Shape on Sensing Performance of Linear Displacement Sensor Using Thin Inductive Coil and Pattern Guide. *Sensors*, 11, pp. 10522-10533. https://doi.org/10.3390/s111110522

[19] Shoshiashvili, L., Shamatava, I., Kakulia, D., Shubitidze, F., 2023. Design and assessment of a novel biconical human-sized alternating magnetic field coil for MNP hyperthermia treatment of deep-seated cancer. *Cancers*, 15, pp. 1672. doi: 10.3390/cancers15061672

[20] Attaluri, A., Jackowski, J., Sharma, A., Kandala, S. K., Nemkov, V., Yakey, Ch., DeWeese, Th.L., Kumar, A., Goldstein, R. C., 2020. Design and construction of a Maxwell-type induction coil for magnetic nanoparticle hyperthermia. *International Journal of Hyperthermia*, 37, pp. 1–14. doi: 10.1080/02656736.2019.1704448

[21] Matsumi, Y., Kagawa, T., Yano, S., Tazawa, H., Shigeyasu, K., Takeda, Sh., Ohara, T., Aono, H., Hoffman, R.M., Fujiwara T., Kishimoto, H., 2021. Hyperthermia generated by magnetic nanoparticles for effective treatment of disseminated peritoneal cancer in an orthotopic nude-mouse model. *Cell Cycle*, 20, pp. 1122–1133. doi:10.1080/15384101.2021.1919441

[22] Rouni, M.A., Shalev, B., Tsanidis, G., Markakis, I., Kraus, S., Rukenstein, P., Suchi, D., Shalev, O., Samaras, T., 2024. A validated methodological approach to prove the safety of clinical electromagnetic induction systems in magnetic hyperthermia. *Cancers*, 16, p. 621. doi: 10.3390/cancers16030621

[23] Chia, D.K., Demuytere, J., Ernst, S., Salavati, H., Ceelen, W., 2023. Effects of hyperthermia and hyperthermic intraperitoneal chemoperfusion on the peritoneal and tumor immune contexture. *Cancers*, 15, p. 4314. doi: 10.3390/cancers15174314

[24] Maraj, E.N., Shah, S. I., Akbar, Sh. N., Muhammad, T., 2023. Thermally progressive Particle-Cu/Blood peristaltic transport with mass transfer in a Non-Uniform Wavy Channel: Closed-form exact solutions. *Alexandria Engineering Journal*, 74, pp. 453-466 https://doi.org/10.1016/j.aej.2023.05.056

[25] Akbar, Sh. N., Maraj, E.N., Shah, S. I, Muhammad, T., 2024. Nano particle distribution in blood via electroosmotic peristaltic flow in a non-uniform wavy membrane basecapillaries. *Sensors and Actuators A: Physical*, 376, p. 115626. https://doi.org/10.1016/j.sna.2024.115626

[26] Akbar, Sh. N., Akram, J., Hussain, M. F., Maraj, E.N., Muhammad, T., 2024. Thermal storage study and enhancement of heat transfer through hybrid Jeffrey nanofluid flow in ducts under peristaltic motion with entropy generation.*Thermal Science and Engineering Progress*, 49, p. 102463. https://doi.org/10.1016/j.tsep.2024.102463

[27] Akram, J., Akbar, Sh. N., Pervaiz, H., Mehmood, R., 2024. Numerical exploration of electroosmotically regulated squeezing rotating flow of TiO_2/water nanofluid in a parallel plate channel under triple diffusion convection. *Physica Scripta*, 99, p. 075249. https://doi.org/10.1088/14024896/ad56d7

[28] Akbar, Sh. N., Akram, J., Hussain, M. F., Maraj, E.N., Muhammad, T., 2024. Hybrid nanofluid flow and heat transfer in symmetric porous ducts with CuO nanoparticles and multi-walled carbon nanotubes under peristaltic motion. *Modern Physics Letters BVol.*, 38, p. 2450333. https://doi.org/10.1142/S0217984924503330

[29] Akbar, Sh. N., Habib, M.B., Rafiq, M., Muhammad, T., Alghamdi, M., 2024. Biological structural study of emerging shaped nanoparticles for the blood flow in diverging tapered stenosed arteries to see their application in drug delivery. *Microfluidics and Nanofluidics*, 28(40). https://doi.org/10.1007/s10404-024-02735-x

[30] Shokri, A.J., Tavakoli, M. H., Sabouri Dodaran A.A., Akhoundi Khezrabad, M.S., 2016. Numerical study of the influence of coil step on the induction heating process in three-dimensional. *Journal of Applied Electromagnetics*, 4, pp. 37-44.

[31] Rosensweig, R.E., 2002. Heating magnetic fluid with alternating magnetic field. *Journal of Magnetism and Magnetic Materials*, 252, pp. 370–374. doi: 10.1016/S0304-8853(02)00706-0

[32] Pennes, H.H., 1948. Analysis of tissue and arterial blood temperatures in the resting human forearm. *Journal of Applied Physiology*, 1(2), pp. 93-122. doi: 10.1152/jappl.1948.1.2.93

[33] Inman, B.A., Etienne, W., Rubin, R., Owusu, R.A., Oliveira, T.R., Rodriques, D.B., Maccarini, P.F., Stauffer, P.R., Mashal, A., Dewhirst, M.W., 2013. The impact of temperature and urinary constituents on urine viscosity and its relevance to bladder hyperthermia treatment. *International Journal Hyperthermia*, 29. https://doi.org/10.3109/02656736.2013.775355

[34] Kell Density, G.S., 1975. Thermal expansivity and compressibility of liquid water from 0° to 150°C: correlations and tables for atmospheric pressure and saturation reviewed and expressed on 1968 temperature scale. *Journal of Chemical & Engineering Data*, 20, pp. 97–105.

[35] Giustini, A. J., Petryk, A. A., Cassim, Sh.M., Tate, J. A., Baker, I., Jack Hoopes, P., 2010. Magnetic nanoparticle hyperthermia in cancer treatment. *Nano Life*, 1. https://doi.org/10.1142/S1793984410000067

[36] Dürr, S., Janko, C., Lyer, S., Tripal, P., Schwarz, M., Zaloga, J., Tietze, R., Alexiou, C., 2013. Magnetic nanoparticles for cancer therapy. *Nanotechnology Reviews*, 2, pp. 395–409. https://doi.org/10.1515/ntrev-2013-0011

[37] Rudnev, V., Loveless, D., Cook, R.L., 2017. *Handbook of Induction Heating*. 2nd ed. CRC Press, Boca Raton.

[38] Stoll, A. M., Greene, L.C., 1959. Relationship between pain and tissue damage due to thermal radiation. *Journal of Applied Physiology*, 14, pp. 373–382. https://doi.org/10.1152/jappl.1959.14.3.373

[39] Petra Kok, H., Korshuize- van Straten, L., Bakker, A., de Kroon- Oldenhof, R., Geijsen, E.D., Lukas, Stalpers, J.A., Crezee, J., 2017. Online adaptive hyperthermia treatment planning during locoregional heating to suppress treatment-limiting hot spots. *International Journal of Radiation Oncology*Biology*Physics*, 99, pp. 1039–1047. https://doi.org/10.1016/j.ijrobp.2017.07.011

[40] Schooneveldt, G., Leijsen, Y.V., Balidemaj, E., Crezee, H., 2018. Clinical validation of a novel thermophysical bladder model designed to improve the accuracy of hyperthermia treatment planning in the pelvic region. *International Journal of Hyperthermia*, 35, pp. 383-397. doi: 10.1080/02656736.2018.1506164